Department of Materials Science and Engineering

Thermodynamic Measurements on Alloys and Compounds in Ag-Au-Se and Ag-Pd systems by the Electromotive Force Method

Dawei Feng

Aalto University

DOCTORAL DISSERTATIONS

Aalto University publication series
DOCTORAL DISSERTATIONS 172/2014

Thermodynamic Measurements on Alloys and Compounds in Ag-Au-Se and Ag-Pd systems by the Electromotive Force Method

Dawei Feng

A doctoral dissertation completed for the degree of Doctor of Science in Technology to be defended, with the permission of the Aalto University School of Chemical Technology, at a public examination held at the lecture hall V1 of the school on 28 November 2014 at 12.

Aalto University
School of Chemical Technology
Department of Materials Science and Engineering
Metallurgical Thermodynamic and Modelling Research Group

Supervising professor
Professor Pekka Taskinen

Thesis advisor
Professor Pekka Taskinen

Preliminary examiners
Professor Herbert Ipser, University of Vienna, Austria
Professor E. G. Osadchii, Russian Academy of Sciences, Russia

Opponent
Doctor Daniel Lindberg, Åbo Akademi, Finland

Aalto University publication series
DOCTORAL DISSERTATIONS 172/2014

ISBN 978-952-60-5934-1 (printed)
ISBN 978-952-60-5935-8 (pdf)
ISSN-L 1799-4934
ISSN 1799-4934 (printed)
ISSN 1799-4942 (pdf)
http://urn.fi/URN:ISBN:978-952-60-5935-8

Unigrafia Oy
Helsinki 2014

Finland

441 697
Printed matter

Aalto University

Abstract

Aalto University, P.O. Box 11000, FI-00076 Aalto www.aalto.fi

Author
Dawei Feng

Name of the doctoral dissertation
Thermodynamic Measurements on Alloys and Compounds in Ag-Au-Se and Ag-Pd systems by the Electromotive Force Method

Publisher School of Chemical Technology

Unit Department of Materials Science and Engineering

Series Aalto University publication series DOCTORAL DISSERTATIONS 172/2014

Field of research Metallurgy

Manuscript submitted 1 August 2014 **Date of the defence** 28 November 2014

Permission to publish granted (date) 28 October 2014 **Language** English

☐ **Monograph** ☒ **Article dissertation (summary + original articles)**

Abstract

Gold and silver chalcogenides are significant minerals and major carriers of precious metals, and silver palladium alloy is one of the most important silver alloys with various industrial applications. The Ag-Au-Se ternary system and the Ag-Pd binary system have been investigated by the electromotive force (EMF) method in this study.

For the Ag-Au-Se ternary system, the numerical values of the standard thermodynamic functions of the compounds Ag_2Se (naumannite), AuSe, and Ag_3AuSe_2 (fischesserite) have been determined by the EMF method in a solid-state galvanic cell with superionic conductor $RbAg_4I_5$ and AgI as solid state electrolyte. The compounds Ag_2Se, AuSe, and Ag_3AuSe_2 were synthesized from pure elements in evacuated quartz glass ampoules and then examined to be homogenous by Scanning Electron Microscope (SEM) and Energy-Dispersive X-ray Spectroscopy (EDS). According to the experimental data on the EMF versus temperature, the analytical equations were obtained for the polymorphic forms of the compounds Ag_2Se, AuSe, and Ag_3AuSe_2. The temperature-dependent relationships of the Gibbs energy of formation on the compounds Ag_2Se, AuSe and Ag_3AuSe_2 in their polymorphic forms and the standard thermodynamic functions of the compounds within the temperature range were also obtained.

For the Ag-Pd binary system, thermodynamic measurements of silver-palladium binary alloys have been performed over the temperature range 450–750 K by the EMF method with the superionic conductor AgI as the solid electrolyte. The activity and partial molar Gibbs energy of silver were obtained for Ag-Pd alloys over the whole composition range and the thermodynamic properties of palladium were calculated using the Gibbs-Duhem equation. The results show that chemical activities of silver exhibit negative deviations over most of the composition range, and the activities of palladium are characterized by both negative and positive deviations from the ideal Raoultian behavior. The results also show the minimum integral enthalpy of mixing on Ag-Pd alloys is located at 60 at.% Ag.

The thermodynamic properties of the Ag-Au-Se ternary system and the Ag-Pd binary system obtained are significant for the production and recycling of precious metals. Moreover, the EMF method has been improved by advanced cell design, gas purification system, as well as temperature measurement, which can be used as an experimental tool for thermodynamic measurement for other alloys and compounds.

Keywords Electromotive force method, Gibbs energy, Entropy, Enthalpy

ISBN (printed) 978-952-60-5934-1 **ISBN (pdf)** 978-952-60-5935-8

ISSN-L 1799-4934 **ISSN (printed)** 1799-4934 **ISSN (pdf)** 1799-4942

Location of publisher Helsinki **Location of printing** Helsinki **Year** 2014

Pages 100 **urn** http://urn.fi/URN:ISBN:978-952-60-5935-8

Preface

This work was executed at the Metallurgical Thermodynamics and Modelling Research Group in the Department of Materials Science and Engineering of Aalto University, Espoo, Finland, between 2011 and 2014.

First of all, I would like to express my deepest gratitude to Professor Pekka Taskinen, for his excellent guidance, distinguished supervision, enormous support and endless patience during my doctoral study. This work would have never been accomplished without help from him. Secondly, I would also like to thank Emeritus Professor Lauri Holappa and Professor Rauf Eric for their kind encouragements and advice for my work. My thanks also go to my colleagues, especially Fiseha Tesfaye and Markus Aspiala, for their help in my experiments. I thank Dr. David Lloyd from physical chemistry laboratory for making the language check of the dissertation.

This work was carried out as a sub task of the ISS (Improved Sulphide Smelting) project under ELEMET (Energy and Lifecycle Efficient Metal Processes) Program of FIMECC (Finnish Metals and Engineering Competence Cluster), supported financially by Tekes (Finnish Funding Agency for Technology and Innovation**)** and also by Boliden Harjavalta, Boliden Kokkola, Norilsk Nickel, as well as Outotec. Financial support from China Scholarship Council (CSC) and the Research Foundation of Helsinki University of Technology are greatly acknowledged.

Finally I would like to thank my parents, who always encourage me to embrace the challenges in my life. I am also grateful to Dr. Håkan Granberg and Judy J. Christian-Granberg for introducing me to study in Finland. The dissertation is dedicated to my father, YongLin Feng.

November 28, 2014

Otaniemi, Espoo, Finland

Dawei Feng

List of Publications

This dissertation consists of a compendium and the following publications, which are referred to in the text by their Roman numerals.

I. D. Feng, P. Taskinen, F. Tesfaye, Thermodynamic stability of Ag_2Se from 350 to 500 K by a solid state galvanic cell, Solid State Ionics. 231 (2013) 1-4.

II. D. Feng, P. Taskinen, Thermodynamic properties of Ag_3AuSe_2 from 300 to 500 K by a solid state galvanic cell, Journal of Alloy and Compounds. 583 (2014) 176-179.

III. D. Feng, P. Taskinen, Thermodynamic stability of AuSe from 400 to 700 K by a solid state galvanic cell, Journal of Chemical Thermodynamics. 71 (2014) 98-102.

IV. D. Feng, P. Taskinen, Thermodynamic properties of Ag_3AuSe_2, submitted to Physics and Chemistry of Minerals.

V. D. Feng, P. Taskinen, Thermodynamic properties of silver-palladium alloys determined by a solid state electrochemical method, Journal of Materials Science, 49 (2014), 5790-5798.

Author's contribution

Publication I: "Thermodynamic stability of Ag_2Se from 350 to 500 K by a solid state galvanic cell"

The author defined the research plan together with the co-authors, performed the literature survey, carried out the experimental work, and analyzed the experimental data. The author wrote the draft of the manuscript, and edited the final version based on the insightful comments from the co-authors.

Publication II: "Thermodynamic properties of Ag_3AuSe_2 from 300 to 500 K by a solid state galvanic cell"

The author defined the research plan together with the co-author, performed the literature survey, carried out the experimental work, analyzed the experimental data. The author wrote the draft of the manuscript, and edited the final version based on the input from the co-author.

Publication III: "Thermodynamic stability of AuSe from 400 to 700 K by a solid state galvanic cell"

The author defined the research plan together with the co-author, performed the literature survey, carried out the experimental work, analyzed the experimental data. The author wrote the draft of the manuscript, and edited the final version based on the input from the co-author.

Publication IV: "Thermodynamic properties of Ag_3AuSe_2"

The author defined the research plan together with the co-author, performed the literature survey, and carried out the major calculation work. The author wrote the draft of the manuscript, and edited the final version based on input from the co-author.

Publication V: "Thermodynamic properties of silver-palladium alloys determined by a solid state electrochemical method"

The author defined the research plan together with the co-author, performed the literature survey, carried out the experimental work, analyzed the experimental data. The author wrote the draft of the manuscript, and edited the final version based on the input from the co-author.

List of Symbols and Abbreviations

Symbols

a	activity
c	Heat capacity
E	Electromotive force value
F	Faraday constant
G	Gibbs energy
$\boldsymbol{G^0}$	Standard Gibbs energy
$\boldsymbol{\Delta_r G}$	Gibbs energy of reaction
H	Enthalpy
P	Pressure
R	Gas constant
S	Entropy
T	Temperature
W	Work
x	Mole fraction
z	Valence number
μ	Chemical potential

Abbreviations

CALPHAD	CALculation of PHAse Diagrams
DTA	Differential Thermal Analysis
EDS	Energy-dispersive X-ray Spectroscopy
EHTB	Extended Hückel Tight-Binding
EMF	Electromotive Force
KC/MS	Knudsen Cell Mass Spectrometry
MGI	Materials Genome Initiative
SEM	Scanning Electron Microscope
SGTE	Scientific Group Thermodata Europe
XRD	X-ray Diffraction

Table of Contents

1. Introduction

1.1 Background

In order to accelerate the pace of materials research, the Materials Genome Initiative (MGI) [1] was launched in United States in 2011. Experimental tools, together with computational tools and digital data, are the central part of this project, which can be seen in figure 1-1.

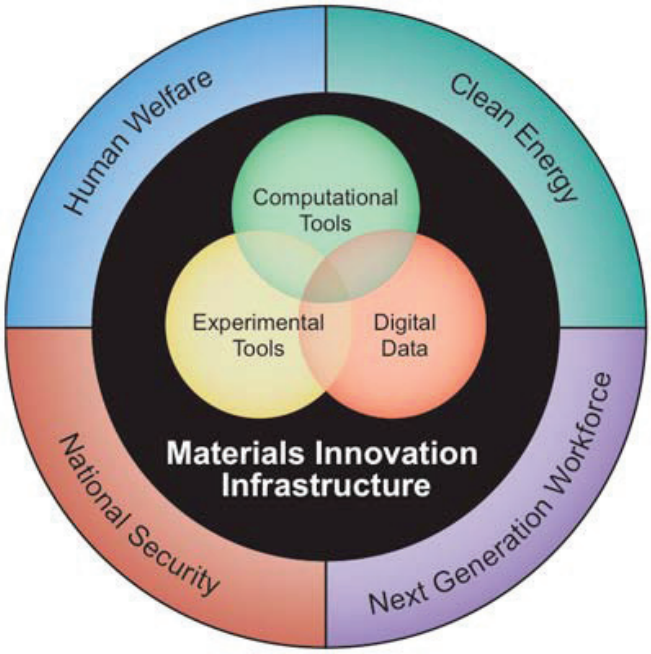

Fig. 1-1. Overview of Materials Genome Initiative (MGI) [1]

The conventional experimental methods for thermodynamic investigation consist of calorimetric method, vapor pressure method, equilibria method, as well as electromotive forces (EMF) method [2]. The EMF method has proved to be direct, effective, and most accurate for the determination of molar Gibbs energy change of reactions [3]. In this work, the EMF method has been employed as an experimental tool to investigate the thermodynamic properties of the Ag-Au-Se ternary and Ag-Pd binary systems.

1.2 The Ag-Au-Se system

The Ag-Au-Se system consists of three binary systems and one ternary system as shown in figure 1-2, where the Ag-Au binary system is solid solution. The Ag-Se and Au-Se binary systems and Ag-Au-Se ternary system will be reviewed briefly in the following section.

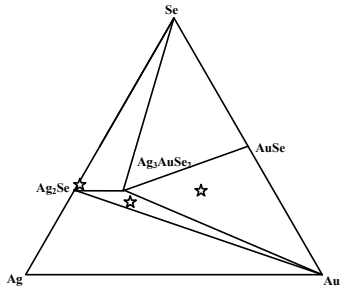

Fig. 1-2. Phase relations in the Ag-Au-Se system with the investigated cell composition shown using the symbol ☆

1.2.1 The Ag-Se system

Ag_2Se is the only intermetallic compound in the Ag-Se binary system. It exhibits excellent magneto-resistance properties and can be used in magnetic field sensors [4, 5]. Ag_2Se is also a byproduct of the electrolytic refining of copper [6]. Therefore the thermodynamic properties of Ag-Se are significant in both the fabrication of magnetic field sensors and smelting processes of copper anode slimes.

The polymorphism of silver selenide was first found by Bellati and Lussana [7] in 1888. The high-temperature structure was determined to be body-centered cubic by Rahlfs [8], while polymorph naumannite [9] forms with an orthorhombic structure [10] at ambient temperatures. A sharp change in resistivity occurs when Ag_2Se is transformed from the low-temperature orthorhombic form (α - Ag_2Se) to the high-temperature body centered-cubic form (β - Ag_2Se) [11].

Various methods have been used to determine the thermodynamic properties of silver selenide. Calorimetry was used by Banus [11], Shukla et.al. [12] and Gronvold et.al. [13], and the vapor pressure method was applied by Scardala et al. [14]. The EMF method is deemed to be direct, effective, and most accurate for the determination of thermodynamic

properties of reactions [15]. The solid electrolyte AgI was first used in EMF measurements on silver selenide by Kiukkola and Wagner [15]. Later, $RbAg_4I_5$ was applied by Takahashi and Yamanoto [16] due to its excellent ionic conductivity. Molten salt electrolyte, such as LiCl-KCl, was also employed by Nasar and Shamsuddin [17]. Coulometric titration was used by Von. Oehsen and Schmalzried [18], Beck and Janek [19] for silver selenide investigation. Recently, Voronin and Osadchii [20] used both solid and liquid electrolytes to investigate the thermodynamic properties of silver selenide. However, the available literature data on the thermodynamic properties obtained in different laboratories are inconsistent. Therefore, it is necessary to carefully study the thermodynamic properties of the Ag-Se system.

1.2.2 The Au-Se system

The gold-selenium system was investigated by Cranton and Heyding [21] in 1968 using differential thermal analysis (DTA) and X-ray powder diffraction (XRD) technique. AuSe is the only known intermetallic phase in the Au-Se system and it was reported to exist in two polymorphs. β-AuSe transformed slowly to α-AuSe above 643 K [21]. Both modifications decompose at 673 K to solid gold and liquid selenium, and form a monotectic phase assembly at 1027 K. Rabenau et al. [22] investigated the Au-Se system in 1971 using the Knudsen effusion method. They calculated the properties of AuSe from selenium pressure ($Se_2(g)$) data, and constructed a complete phase diagram. The thermodynamic data have been compiled by Olin et al. [23].

The crystal structures of AuSe were described by Rabenau et al. [24] in 1976, and the results were refined by Cretier and Wiegers [25], who proposed its structure as mixed valence $(Au^{3+},Au^{+})Se^{2-}$. The polymorphic forms of AuSe have been studied recently using Mössbauer spectroscopy by Wagner et al. [26], combined with ab initio calculation using WIEN 2K software. Lee et al. [27] made EHTB (extended Hückel tight-binding) calculation and results confirm the proposed (Au^{3+}, Au^{+}) (Se^{2-}) structure. However, X-ray absorption data by Ettema et al. [28] prove that Au atoms in AuSe are all in the monovalent state. The phase diagram was provided by H. Okamoto and T. B. Massalski [29].

1.2.3 The Ag-Au-Se system

The Ag_3AuSe_2 is one of the ternary silver gold chalcogenides and exists in nature as fischesserite, which was discovered by Johan et al.[30]. By electron microprobe and physical characterization, they deduced fischesserite is the selenium analogue of petzite. More recently, the structural and physical properties for fischesserite have been investigated by Bindi et al.[31]. They confirmed that fischesserite is topologically identical to petzite, apart from the slight differences in the size of the anions.

The electronic and ionic conduction of the pseudo-binary system $Ag_{2-x}Au_xSe$ ($0 \leq x \leq 0.5$) was first investigated by Wiegers [32] through differential thermal analysis (DTA) and Guinier-Lenne High Temperature X-Ray Camera. Two ordered compounds α-Ag_2Se and α-Ag_3AuSe_2 were found at low temperatures. Sakai et al. [33] and Wagner et al. [34] measured the ternary silver gold chalcogenides by Mössbauer spectroscopy and suggested that the gold in the compound should be considered as monovalent. Fang et al. [35] made band structure calculations for the low temperature modification of the silver chalcogenide α-Ag_3AuSe_2 and the results show that α-Ag_3AuSe_2 is a semiconductor with an energy gap of 0.2 eV.

Tavernier et al. [36] investigated Ag_3AuSe_2 by DTA and found the phase transition temperature to be 543 K. Later, Smit et al. [37] studied by X-ray diffraction (XRD) and DTA and found the phase transition temperature to be 540 K. They found the melting point of Ag_3AuSe_2 to be at 1000 K. Prince [38] reviewed the Ag-Au-Se system in 1988. However, the thermodynamic properties of Ag_3AuSe_2 at low temperatures remain poorly studied. Recently, Osadchii et al. [39] investigated the Ag-Au-Se system below 405 K. Nevertheless, enlarging the temperature range can help prove the results and may bring us a better understanding of the thermodynamic behavior of Ag_3AuSe_2, owing to the fact that the solid state electrolyte $RbAg_4I_5$ does not melt until 500 K [40].

1.3 The Ag-Pd system

Silver palladium alloy is one of the most important silver alloys with various industrial applications, such as hydrogen permeation [41], hydrogen storage [42] and lead-free soldering [43].

The phase diagram of the binary Ag-Pd system was first determined by Ruer [44] through thermal analysis, and it is characterized by complete miscibility in the solid and liquid state. The crystal structure for silver-palladium alloys was determined by McKeehan [45] to be face-centered cubic (fcc) through X-ray diffraction (XRD), and the crystal lattice parameter was found to vary with nearly linear function of the atomic percentage. Later, Coles [46] investigated the lattice spacing of Ag-Pd alloys, and he found a marked change in the slope of the lattice spacing vs. composition curve near 60% silver. Hoare and Yates [47] measured the low temperature specific heats of Ag-Pd alloys from 2 to 4.2 K and obtained the Debye temperature and the electronic heat coefficient.

Electromotive force (EMF) method was used by Pratt [48], where a molten salt mixture of KCl and NaCl was chosen as electrolyte with small amounts of AgCl. The Gibbs free energies of mixing and activities were obtained at 1000 K. Later on, Raychaudhuri [49] studied the thermodynamic properties of solid silver-palladium alloys by EMF method over the temperature range of 850 to 1150 K, with beta alumina containing substituted silver ions as a solid electrolyte. The activity of silver at 1000 K was found to obey a negative deviation from Raoultian behavior over most of the composition range. The large negative excess entropies observed were discussed in terms of non-configurational changes by alloying. Thus, the major contribution to the thermodynamic properties of the Ag-Pd system was attributed to be electronic in origin.

Calorimetry was employed by Oriani and Murphy [50] to measure the heat of mixing of Ag-Pd alloy at 915 K. They found that the Ag-Pd alloys were characterized with very large negative enthalpies and excess entropies of mixing and explained the phenomena with the changes in electronic, vibrational and paramagnetic properties. Later, Chan and Hultgren [51] investigated the thermodynamic properties of Ag-Pd alloy by liquid tin solution calorimetry. They found the minimum enthalpy of mixing is located at a mole fraction 0.40 of palladium, which was attributed to the magnetic character of the alloy. The Ag-Pd alloys are diamagnetic below a mole fraction 0.4 of palladium and paramagnetic above. Recently, Luef et al. [52] investigated the binary liquid Ag-Pd alloys with compositions up to 55 at.% Pd at 1673 K using a drop calorimetric technique.

They found that all measured enthalpies of mixing are exothermic with pure liquid metals as standard state, and the fitted curve shows a minimum at 35 at.% Pd.

Torsion effusion method was used by Myles [53] to investigate the Ag-Pd alloys over a temperature range of 1100-1300 K. The activities of silver were found to exhibit a large negative deviation from the ideal Raoultian behavior over the entire compositional range and the minimum enthalpy of mixing is located at a mole fraction 0.60 of silver. The results were later confirmed by Eremenko et al. [54] by using the Knudsen effusion cell. Schmahl [55] investigated the Ag-Pd alloys and obtained the activity data of palladium by using a chemical equilibration method. Savitskii and Pravoverov [56] found the change of physical properties versus composition of the quenched and annealed alloys, and suggested that the Pd-Ag system forms intermetallic compounds corresponding to the stoichiometric compositions of Ag_2Pd_3 and AgPd. However, the super-structural lines could not be detected by XRD, which is attributed to the similar atomic scattering factors of palladium and silver.

Experimental data of the binary Ag-Pd system were compiled by Karakaya and Thompson [57]. Thermodynamic modeling of the Ag-Pd system was made by Ghosh et al. [43], where the Ag-Pd phase diagram, enthalpies of mixing and activities were assessed. However, Sopousek et al. [58] found there is substantial discrepancy in the enthalpy of mixing of liquid Ag-Pd alloys between the available experiments [52] and modeling [43]. Thus, they made a reassessment of the Ag-Pd system based on their experimental work by DSC, coupled with Knudsen cell mass spectrometry (KC/MS). Nevertheless, experimental data on the thermodynamic properties of Ag-Pd system below 700 K are still scarce.

1.4 Objectives

The first objective of this study is to improve the EMF method as an experimental tool for thermodynamic measurements by advanced cell design, gas purification as well as temperature measurement. The second objective of the present study is to determine experimentally the thermodynamic properties of Ag-Au-Se (Publication I-IV) and Ag-Pd (Publication V) system, by using EMF measurements in solid-state galvanic cells.

In the following section, the EMF method will firstly be described in detail in chapter 2 and chapter 3. Then the thermodynamic measurements of the Ag-Au-Se and Ag-Pd system will be shown in chapter 4 and chapter 5. Finally the EMF method and thermodynamic data obtained will be discussed in chapter 6 and finally conclusions are given in chapter 7.

2. Electromotive force method

In this work, the EMF method has been chosen as the experimental tool for thermodynamic investigation, and will be discussed in this section.

2.1 Principles

The basic electrochemical cell with solid electrolyte works in the following form,

(-) M (solid or liquid) | ionic conductor on M^{z+} | M in alloy or compounds (+) (A)

where the left side of the equation has pure M component as a reference electrode, and the right side has an alloy or compounds of a multicomponent system as working electrode.

For any chemical process occurring under constant *P* and *T*, the maximum work in a reversible process that can be done by the system is equal to the decrease in its Gibbs free energy:

$$W = -\Delta G \tag{2-1}$$

If this work is in electrical form, it equals to the multiplication of the charge passed zF and voltage *E*. For a balanced cell reaction, which brought the transfer of z moles of electrons, this work is given by:

$$W = zFE \tag{2-2}$$

where E is the electromotive force produced by the cell. From the relationships (2-1) and (2-2), the Gibbs energy change of the reversible chemical reaction which takes place inside the cell, can be determined as:

$$\Delta G_r = -zFE \tag{2-3}$$

where z is number of moles of electrons involved in the process and F is Faraday constant (96485.34 C mol^{-1}). Using the relations between ΔG, ΔH and ΔS, one can express corresponding enthalpy and entropy changes through the E vs. T dependence as:

$$\Delta S = zF\left(\frac{\partial E}{\partial T}\right)_P, \tag{2-4}$$

$$\Delta H = zF\left[\left(T \cdot \left(\frac{\partial E}{\partial T}\right) - E\right)\right]_P, \quad (2\text{-}5)$$

Thus, from the measured E versus T dependence, thermodynamic functions of the well-defined chemical process can be derived. Any meaningful thermodynamic investigation requires that the cell functions in a reversible way, i.e., that no external current is flowing. This is assured by the use of high-impedance (larger than 10^{10} Ω) measuring devices in this study, resulting in the measurement of an open-circuit potential.

The main successful factors for a cell operation are to find a suitable electrolyte and the exact identification of the single reversible process occurring at each electrode. The corresponding electrolyte should provide superionic conductivity in the temperature range, i.e., one single ion should be responsible for establishing the potential. In this study, the following efforts have been made in order to make the cell work successfully,

1. Reactions between electrodes and lead wires can be avoided by using inert platinum as lead wire;
2. Temperature gradients in the cell can be avoided by the isothermal zone;
3. Reactions between crucible materials and electrodes or electrolyte can be neglected in solid state;
4. Stable EMF values can be obtained as an indication of equilibria;
5. Direct exchange of matter between the two electrodes (e.g., via the gas phase) can be excluded in solid state; and
6. Reaction with the atmosphere can be avoided by using pure argon as gas flow.

2.2 Solid state electrolyte

In this study, α-AgI and $RbAg_4I_5$ have been employed as solid state electrolytes for thermodynamic investigation of silver alloys and compounds based on their physical and chemical properties.

2.2.1 α-AgI

The polymorphic relationship of silver iodide at atmospheric pressure has been investigated by Burley [59] using high temperature X-ray diffraction (XRD) and differential thermal analysis (DTA) techniques. A hexagonal (wurtzite type) and a face-centered cubic (zincblende or sphalerite type) phase can exist up to 420 K, while the

latter is metastable over this entire range. From 420 K to the melting point 828 K, only disordered body-centered cubic phase α-AgI can exist.

α-AgI was found to have a high conductivity of 1 $S \cdot cm^{-1}$ in 1914 by Tubandt and Lorentz [60]. In the temperature range from 420 K to melting temperature 828 K, ionic conductivity of α-AgI monotonously increases until its melting point. Patterson [61] has shown that the chemical potential of silver in AgI changes only slightly based on various conductivity data and EMF data. Fiseha et al. [62] have calculated the activity of silver (a_{Ag}) in AgI at $P_{I_2(g)}$=1 atm (for the dissociation reaction $2AgI=2Ag+I_2(g)$), as a function of temperature. According to the results from their analysis, the a_{Ag} in AgI varies between 2.5×10^{-9} at 420 K, 1.2×10^{-7} at 500 K, and 3.6×10^{-5} at 700 K. Thus, the chemical potential of silver in AgI does not change significantly in its ionic conduction domain. Thus the α-AgI is a suitable solid state electrolyte for EMF measurements on silver alloys and compounds from 420 K to 750 K.

2.2.2 $RbAg_4I_5$

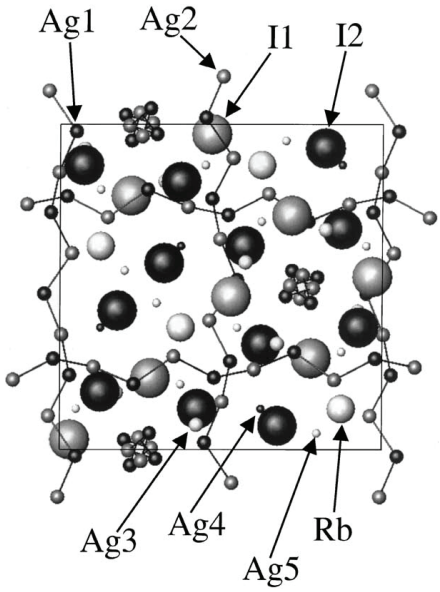

Fig. 2-1. Crystal structure of $RbAg_4I_5$ by Hull et al. [63], reproduced with permission of Elsevier

The crystal structure of the solid electrolyte $RbAg_4I_5$ has been determined by Geller [64] in 1967 from single-crystal x-ray diffraction data. There are four $RbAg_4I_5$ in a cubic unit cell with a = 11.24 Å. The structure refinement, by least squares, is based on space group $P4_13$ (O^7). The arrangement of the iodide ions is similar to that of the manganese atoms in β-manganese, and provides 56 iodide tetrahedra per unit cell, which share faces in such a manner as to provide diffusion paths for the silver ions. The occurrence of the low-temperature phase of $RbAg_4I_5$ has been established by X-ray diffraction and optical examination. The crystal structure of $RbAg_4I_5$ can be seen in Fig. 2-1.

The high ionic conductor $RbAg_4I_5$ was independently discovered by Bradley and Greene [65] and Owens&Argue [40]. Bradley and Greene [65] determined the phase diagram for the RbI-AgI binary system. There exists a stable intermetallic compound $RbAg_4I_5$ with incongruent melting points at 500 K. High conductivity was found in $RbAg_4I_5$. Owens and Argue [40] report the conductivity results for the compounds of the group $RbAg_4I_5$, where they have observed the conductivity can reach as high as 0.21 S/cm at room temperature.

Therefore the $RbAg_4I_5$ is a suitable solid state electrolyte for EMF measurement of silver alloys and compounds from room temperature to its incongruent melting point of 500 K.

2.3 Operation conditions

In order to guarantee that the EMF cells work, the operating conditions in this study were obeyed and summarized as following,

1. Temperature range: AgI operates at 420-750 K and $RbAg_4I_5$ at 300-500 K;
2. Atmosphere: EMF cell is protected in a purified argon atmosphere;
3. EMF measurement: reversible reaction is achieved by an impedance of $2 \cdot 10^{14}$ Ω;
4. Isothermal zone: the temperatures of both ends of EMF cell were measured;
5. Equilibria reached: stable EMF values are obtained after long operating time.

3. Experimental

3.1 Materials synthesis and characterization

3.1.1 Silver alloys and compounds

The silver chalcogenides Ag_2Se, AuSe, and Ag_3AuSe_2 were prepared by a direct synthesis from the elements, where the gold powder from Alfa Aesar (99.99% in purity), silver powder from Alfa Aesar (99.99 % in purity) and selenium powder from Koch-Light Laboratories Ltd (99.999 % in purity) were used.

For the compound Ag_2Se, the Ag and Se powder were mixed together in a mole ratio of 2:1 and sealed in an evacuated quartz glass ampoule. Then the ampoule was heated up from room temperature to 673 K at a rate of 4 K/min and kept at that temperature for 2 days. After that it was heated to 873 K and then kept at that temperature for 2 days. Finally, it was heated to 1173 K (the melting point of Ag_2Se), and kept there for one hour, and then cooled down to room temperature.

For the compound AuSe, the Au and Se powder were mixed together in a mole ratio of 1:1 and sealed in an evacuated fused quartz glass ampoule. Then the ampoule was heated up from room temperature to 673 K at a rate of 4 K/min, and kept at that temperature for 1 week. After that it was cooled down to 623 K and kept for 1 week. Finally, it was cooled down to room temperature.

For the ternary compound Ag_3AuSe_2, the materials were synthesized from elements in stoichiometric compositions using evacuated quartz glass ampoules according to the method of Rabenau et al. [24]. The synthesis was carried out in a vertical resistance heated tube furnace. During synthesis of selenide, the ampoules were annealed for 3–4 days at 673 K to ensure reaction of the elements; afterwards, the temperature was raised to 1273 K and the annealing continued for 1–2 days at this temperature. Then the ampoules were cooled down slowly to room temperature in the furnace over one week and unsealed.

The Ag-Pd alloys were prepared from 99.97 % pure silver supplied by Outokumpu (Finland) and 99.9 % palladium powder supplied by Alfa Aesar (Germany). The silver

palladium alloys were prepared by melting them in a pure argon atmosphere, and then annealed at 673 K for one day. The alloys were pressed uniaxially to obtain a pellet of 20 mm in diameter and 2 mm in thickness, under pressure of 0.1 GPa.

The Ag_2Se and AuSe compounds and Ag-Pd alloys were examined to be homogenous by SEM (LEO 1450), and EDS (Oxford instruments, UK). The ternary compound Ag_3AuSe_2 were characterized to be fischesserite phase by Panalytical X'Pert Pro MRD (Philips, Netherland) using Co-K_α radiation.

3.1.2 Electrolytes

The solid electrolyte, $RbAg_4I_5$, was synthesized according to the method described by Owens and Argue [40]. Weighing of 0.8 mole fraction of silver iodide from Alfa Aesar (99.9 % in purity, Germany) and 0.2 mole fraction of rubidium iodide from Alfa Aesar (99.8 % in purity, Germany) was followed by mixing. The mixture was sealed in a glass tube under vacuum, and heated at 493 K for 2 hours. Then after being cooled down and maintained at 433 K for 15 hours, the solid state electrolyte $RbAg_4I_5$ was obtained.

The electrolyte AgI was supplied by Alfa Aesar in 99.999 % purity (Germany). In addition, platinum (99.9%, Johnson-Matthey, UK) was used as lead wire in the experiment.

3.2 Apparatus

The experimental setup for the EMF measurements consists essentially of the following module: (I) constant temperature profile; (II) cell assembly; (III) gas purification system; (V) measurement system for temperature and voltage; (VI) data recording system and (VII) bubble system at the downstream of the EMF measurement to monitor the continuous gas flow. The details are briefly shown in Fig. 3-1.

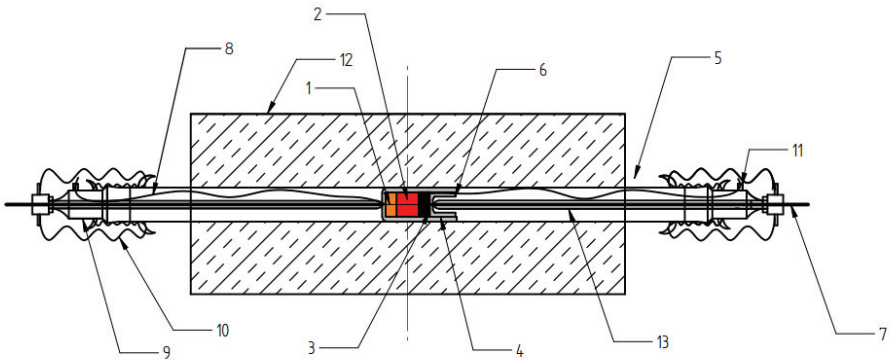

Fig. 3-1. Schematic illustration of apparatus, (1) reference electrode, (2) electrolyte, (3) working electrode, (4) alumina crucible, (5) alumina tube, (6) pressure block, (7) moveable platinum resistance thermometer, (8) platinum lead, (9) loading springs, (10) quick-coupling head, (11) inert gas inlet/out, (12) Lenton tube furnace and (13) alumina sheath.

The reference electrode (1), electrolyte (2) and the working electrode (3) form a 'sandwich' that is inside an alumina crucible (4). The alumina crucible (4), with a central hole to pass the platinum lead (8) through, is placed in the center of an outer alumina tube (5) which functions as a holder for the galvanic cell. A thinner alumina crucible (6) is placed on the right of the working electrode (3) as a pressure block. The pressure block is compressed by a moveable platinum resistance thermometer (7) inside an alumina sheath (13). The loading springs (9) exert enough pressure to ensure good electrical contact between the electrolyte and the electrodes. The platinum lead (8) comes out through a small hole near the flat end of the central alumina tube (5). The open end of the alumina tube (5) is attached permanently to a quick-coupling head (10). The platinum resistance thermometers (7) and the platinum leads (8) come out through insulated holes at the quick-coupling heads (10). All these holes are sealed with epoxy resin to make a gas tight assembly. The quick-coupling heads are provided with side tubes (11) to maintain an inert gas flow through the cell. All the above parts are located inside a Lenton tube furnace (12).

3.2.1 Gas purification

Gas flow of dry argon (99.999% in purity) to the EMF cell was further purified before introduction to the cell, by passing through an auxiliary furnace with titanium wire at 900 K for removing oxygen traces. Owing to these improvements, the accuracy of EMF measurement and its stability as a function of time was excellent, allowing very long measuring duration for each experimental cell.

3.2.2 EMF measurements

A Lenton tube furnace (type LTF 12/50/610) was used in the experiments to achieve a constant temperature profile, which was measured by using two moveable resistance thermometers. Schematic illustration of the experimental furnace for carrying out measurements with the solid electrolytes is shown in Fig. 3-1. During the EMF-measurements, temperatures on both ends of the galvanic cell were measured using two PT100 sensors (platinum resistance thermometers, PRT). The PRTs, with tolerance class B 1/10 DIN, i.e. ± 0.03 °C variation at 0 °C, according to the manufacturer, were calibrated in a mixture of ice and water at 0 °C. The obtained resistance values of 100 Ω (R_0 = 100.026 Ω and R_0 = 100.03 Ω, respectively) were inserted to a program based on a LabVIEW software code from National Instruments that records the temperature values from each PRT. The accuracy of temperature and EMF readings were 0.01 K and 0.001 mV, respectively.

Most measurements were performed by heating and cooling the cell in steps from 1 to 10 °C. To reach a steady state EMF reading, the process required anywhere from a few hours up to two weeks. Equilibrium was considered to be reached when the EMF-values were constant, or their variations were not significant (less than 0.1 mV), and they were oscillating at a certain constant value for several hours. Temperature differences between the two electrodes of the EMF cell were controlled within 1 K ($0.1 < T\,(K) < 0.8$), by manually adjusting the horizontal position of the galvanic cells and observing the real-time temperature readings over the cell from highly accurate PRTs. The uncertainties of temperature and EMF were established to be ± 0.5 K and ±0.1 mV, respectively. Thus, the possible thermoelectric effect generated in the cell EMF by temperature gradients was regarded as negligible.

Functionality of the experimental electrochemical system was tested by measuring the EMF of the symmetric cell Ag | Ag^+ | Ag, which theoretically should not result in any measurable EMF or electric potential difference. The equilibria in this study were considered reproducible when the EMF readings in heating and cooling coincided.

In this particular EMF cell design, the sensitive PRT's are connected to each end of the cell, in order to record the temperature exactly on the anode and cathode half cells, thus eliminating temperature difference induced errors in the EMF measurements.

3.2.3 Data recording

Identical platinum wires for the EMF-measurements were used, and the lead wires from the PT100 sensors for temperature measurements were connected to a KEITHLEY-6517B/electrometer/high resistance meter and a KEITHLEY-2000-multimeter, respectively. Input impedance of the electrometer for EMF-measurements was $2 \cdot 10^{14}$ Ω, which allows the cells to function in a reversible way. The measured EMF-values and temperatures were simultaneously transferred to a computer through a IEE-488-GPIB-cable and a KEITHLEY-KUSB-488A USB-to-GPIB interface adapter, and the readings were recorded by the software, giving two measured values every 5 seconds.

3.2.4 EMF cells

The EMF cells have been measured with $RbAg_4I_5$ or AgI as the solid state electrolyte, these are have been summarized in table 3-1.

Table 3-1. Galvanic cells investigated in this study

System	Temperature	Galvanic cell
Ag-Se	350-500 K	(-) Pt | Ag(s) | $RbAg_4I_5$(s) | Ag_2Se(s), Se(s, l) | Pt (+)
Au-Se	400-700 K	(-) Pt | Ag(s) | AgI(s) | Ag_3AuSe_2, AuSe, Au | Pt (+)
Ag-Au-Se	300-500 K	(-) Pt | Ag(s) | $RbAg_4I_5$(s) | Ag_3AuSe_2, Ag_2Se, Au | Pt (+)
Ag-Pd	450-750 K	(-) Pt | Ag(s) | AgI(s) | Ag-Pd alloys (s) | Pt (+)

4. The Ag-Au-Se system

The thermodynamics of the Ag-Au-Se system, including Ag-Se and Au-Se system, will be discussed in this section. The EMF values of the following virtual cell reactions have been measured by EMF method and summarized in the table 4-1.

Table 4-1 Virtual cell reactions in the Ag-Au-Se system

System	Temperature	Cell reaction	
Ag-Se	350-500 K	$2Ag(s)+Se(s)=Ag_2Se(s)$	(4-A)
Ag-Au-Se	300-500 K	$Ag(fcc)+\alpha\text{-}Ag_3AuSe_2=2Ag_2Se+Au(fcc)$	(4-B)
Au-Se	400-700 K	$3Ag(fcc)+2AuSe(s)=Ag_3AuSe_2(cr)+Au(fcc)$	(4-C)

4.1 EMF values

4.1.1 Ag-Se system

The comparison of the EMF measurements obtained by various authors according to the literature sources are shown in Figure 4-1. The observed values of EMF (E, mV) at different temperatures obtained in this study are listed in Appendix A-1.

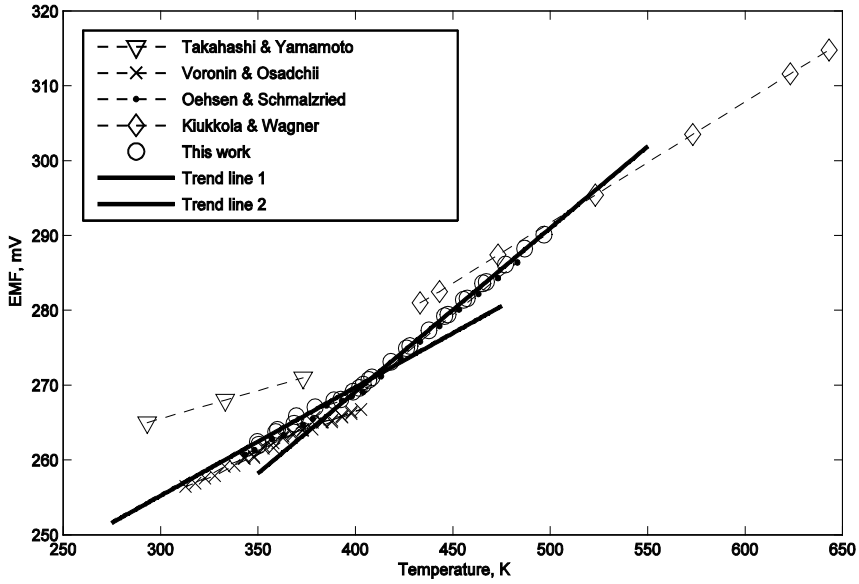

Fig. 4-1. Temperature dependence of EMF for cell reaction $2Ag(s)+Se(s)=Ag_2Se(s)$ from various authors

Our data agrees well with Oehsen and Schmalzried [18] by solid coulometric titration. Moreover, the data obtained in this study confirm the results given by Osadchii and Voronin [20] at lower temperatures, and with Kiukkola and Wagner [15] at higher temperatures above the polymorphic transformation temperature. However, Yamamoto and Takahashi's data [16] below the polymorphic transformation temperature are higher than other author's values. At 373 K, the EMF value difference with other authors can reach 5.2 mV. This may result from the non-equilibrium in the measurement, due to lack of sufficient equilibration time in the observations, which was limited only for a few hours. In fact, the equilibrium of reaction (4-A) was typically reached after 1-2 weeks in the present experimental conditions, resulting from slow diffusion of silver ions at low temperatures [66].

4.1.2 Au-Se system

The obtained results are listed in appendix A-2, and the temperature dependence of the EMF from the virtual cell reaction is shown in Figure 4-2. It displays the experimental data and compares the experimental points with the previous observations [39, 67].

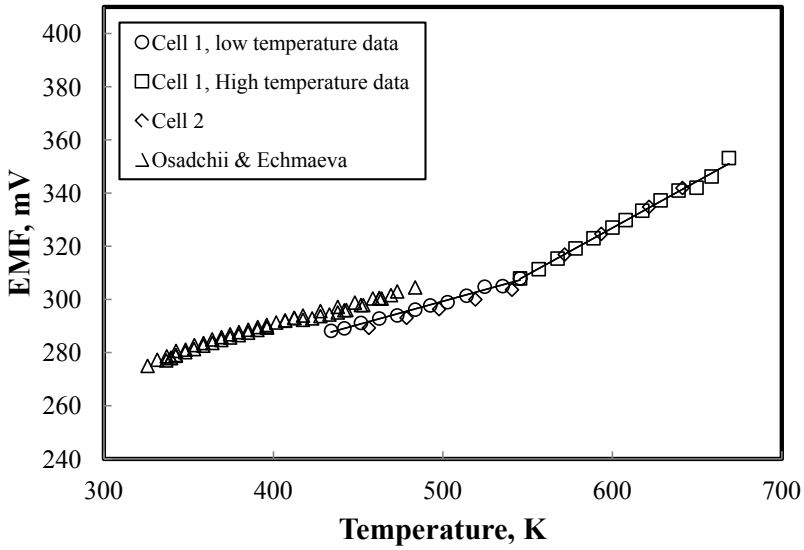

Fig. 4-2. Temperature dependences of EMF for cell reaction $3Ag(fcc)+2AuSe(s)=Ag_3AuSe_2(cr)+Au(fcc)$

In Fig. 4-2, there is apparently a slope change around 550 K indicating a phase transformation occurs in the cell. The polymorphic phase transformation for Ag_3AuSe_2 has been reported to exist at around 540 K by Smit et al. [37]. Therefore phase transformation was considered as from α'-Ag_3AuSe_2 to β-Ag_3AuSe_2 over its experimental temperature range in this study and in the following thermodynamic treatment. More details can be found in Paper III.

4.1.3 Ag-Au-Se system

The observed EMF values are listed in Appendix A-3, and its dependence on temperature is shown in Fig. 4-3. Ag_3AuSe_2 (fischesserite) in equilibrium with Ag_2Se, have been obtained over the temperature range of 300-500 K. The current experimental data suggest that a phase transformation of Ag_3AuSe_2 can been observed at 349.3 K. The temperature was obtained by solving the experimental EMF functions and taking into account the α-β solid state phase transformation of Ag_2Se at 407.7 K. The enthalpy of the phase transformation based on the EMF vs. temperature plot is 5.538±0.764 $kJ \cdot mol^{-1}$. The slope change of the temperature dependence gives thermodynamic evidence for a phase transformation.

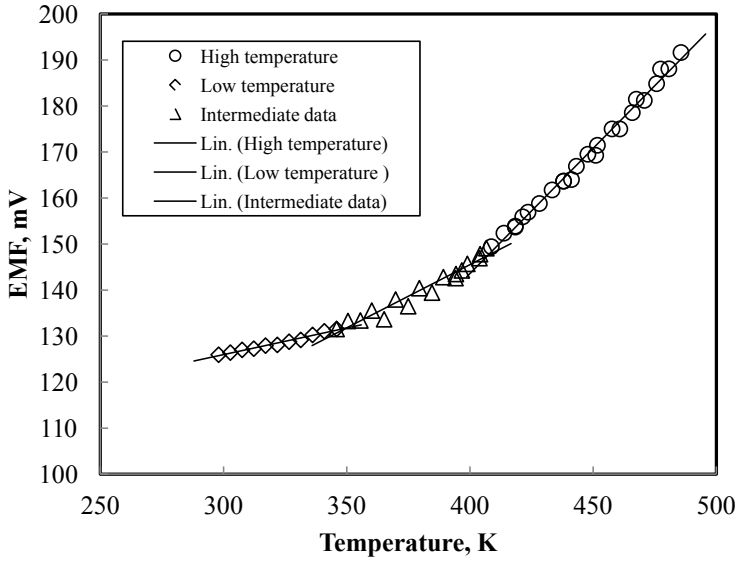

Fig. 4-3. Temperature dependence of EMF for the cell reaction Ag(fcc)+α-Ag_3AuSe_2=2Ag_2Se+Au(fcc)

4.2 EMF dependence of temperature

The analytical equations were obtained by the least square method, using the linear relationship polymorphs E = a + b · T for each. The EMF dependences of temperature are summarized in table 4-2.

Table 4-2 EMF dependence of temperature in the Ag-Au-Se system

Cell reaction	Temperature	EMF dependence of temperature
(4-A)	350-408 K	$E/mV = (211.79 \pm 3.01) + (0.1448 \pm 0.0079) \cdot T/K$
	408-500 K	$E/mV = (181.70 \pm 0.51) + (0.2186 \pm 0.0011) \cdot T/K$
(4-B)	298-350 K	$E/mV = 91.193(\pm 1.823) + 0.116(\pm 0.006) \cdot T/K$
	350-407 K	$E/mV = 35.663(\pm 6.100) + 0.275(\pm 0.016) \cdot T/K$
	407-488 K	$E/mV = -74.052(\pm 4.422) + 0.544(\pm 0.010) \cdot T/K$
(4-C)	430-550 K	$E/mV = 211.503(\pm 2.389) + 0.176(\pm 0.005) \cdot T/K$
	550-700 K	$E/mV = 115.94(\pm 5.515) + 0.352(\pm 0.009) \cdot T/K$

4.3 Gibbs energy of reaction

Based on the data from table 4-2, the Gibbs energy changes of reaction are calculated from the equation (2-3)

$$\Delta G_r = -zFE \tag{2-3}$$

The result can be summarized in Table 4-3.

Table 4-3 Gibbs energy of reaction in the Ag-Au-Se system

Cell reaction	T/K	Gibbs energy of reaction, J/mol
(4-A)	350-408	$\Delta_r G = (211.79 \pm 3.01) + (0.1448 \pm 0.0079) \cdot T/K$
	408-500	$\Delta_r G = (181.70 \pm 0.51) + (0.2186 \pm 0.0011) \cdot T/K$
(4-B)	298-350	$\Delta_r G = -8798.757(\pm 175.892) - 11.192(\pm 0.579) \cdot T/K$
	350-407	$\Delta_r G = -3440.945(\pm 588.559) - 26.533(\pm 1.544) \cdot T/K$
	407-488	$\Delta_r G = 7144.91(\pm 426.657) - 52.488(\pm 0.965) \cdot T/K$
(4-C)	430-550	$\Delta_r G = -61219.7(\pm 691.5) - 50.83(\pm 1.45) \cdot T/K$
	550-700	$\Delta_r G = -33559(\pm 1596.3) - 101.74(\pm 2.61) \cdot T/K$

4.4 Gibbs energy of formation

Based on the data from table 4-3, the standard thermodynamic properties of formation for the crystalline phases in the Ag-Au-Se system at 298.15 K with 1 atmospheric pressure can be calculated and summarized in Table 4-4.

Table 4-4: Standard thermodynamic properties of formation for the crystalline phases in the Ag-Au-Se system at 298.15 K and atmospheric pressure

Phase	$-\Delta_f \boldsymbol{G^0}, \mathbf{kJ\ mol^{-1}}$	$-\Delta_f \boldsymbol{H^0}$, kJ mol^{-1}	$\Delta_f \boldsymbol{S^0}$, J K^{-1}mol^{-1}	Reference
α-Ag_2Se	49.24±0.46	40.869±0.581	27.95±1.53	[Publication I]
β-Ag_2Se	47.43±0.29	35.062±0.099	42.18±0.22	[Publication I]
α-AuSe	5.43±0.56	8.770±1.310	-11.3±2.14	[Publication III]
α-Ag_3AuSe_2	86.344±1.268	72.941±1.336	43.88±1.02	[Publication II]
α-Ag_3AuSe_2	86.398±0.795	75.056±0.974	37.81±1.14	[Publication IV]
α'-Ag_3AuSe_2*	85.54±2.71	69.70±1.74	53.2±3.3	[Publication IV]
α'-Ag_3AuSe_2**	80.24±2.71	56.31±1.74	80.25±3.26	[Publication IV]
β-Ag_3AuSe_2	67.75±6.21	28.65±4.03	131.16±7.23	[Publication IV]

* denotes solid selenium as standard state, ** denotes liquid selenium as standard state.

5. The Ag-Pd system

The thermodynamics of the Ag-Pd system will be discussed in this section. Measurements on Ag-Pd were made as a function of alloy composition and temperature by determining the EMF of the following electrochemical cells,

Ag (s) / AgI (s) / Ag-Pd alloy (s). (A)

The virtual cell reaction, when one mole of silver is transferred from reference to alloy, is the following,

Ag(s, fcc) = Ag[Pd]. (B)

The measured electromotive forces of cell (A) can be used to calculate the partial Gibbs energy of silver or its molar chemical potential in the solid Ag-Pd alloys by

$$E = \frac{-\Delta G_{Ag}}{zF} = -\left(\frac{RT}{zF}\right) \ln a_{Ag[Pd]} \quad (5\text{-}1)$$

where F is the Faraday constant (96485.34 C mol^{-1}), z is the number of elementary charges transferred in the virtual cell reaction (with z=1) and a_{Ag} is the activity of silver in the alloy, referred to pure fcc silver.

5.1 EMF values

The observed temperature dependences of the EMFs for the virtual cell reaction (B) are listed in Appendix B-1 to B-3 and shown in Table 5-1. The analytical equations describing the EMF were obtained by the least squares method, using the linear relationship E/mV = b + c · T/K.

Table 5-1 EMF dependence of temperature in the Ag-Au-Se system

Alloys	Temperature	EMF dependence of temperature
$Ag_{0.99}Pd_{0.91}$	450-650 K	$E/mV = 90.776(\pm 4.411) + 0.0796(\pm 0.0080) \cdot T/K$
$Ag_{0.17}Pd_{0.83}$	450-650 K	$E/mV = 67.032(\pm 4.989) + 0.0853(\pm 0.0089) \cdot T/K$
$Ag_{0.35}Pd_{0.65}$	500-650 K	$E/mV = 19.226(\pm 5.189) + 0.0790(\pm 0.0088) \cdot T/K$
$Ag_{0.60}Pd_{0.40}$	550-700 K	$E/mV = 22.180(\pm 2.864) + 0.0482(\pm 0.0043) \cdot T/K$
$Ag_{0.80}Pd_{0.20}$	298-350 K	$E/mV = 5.029(\pm 1.224) + 0.0198(\pm 0.0019) \cdot T/K$

5.2 Activities

Fig. 5-1 shows the activity data obtained by different authors. Negative deviations from the ideal Raoultian behavior can be found for the activities of silver over most of the composition range. A small positive deviation from Raoultian behavior is found for low-silver alloys, which essentially confirms the results from Raychaudhuri [49].

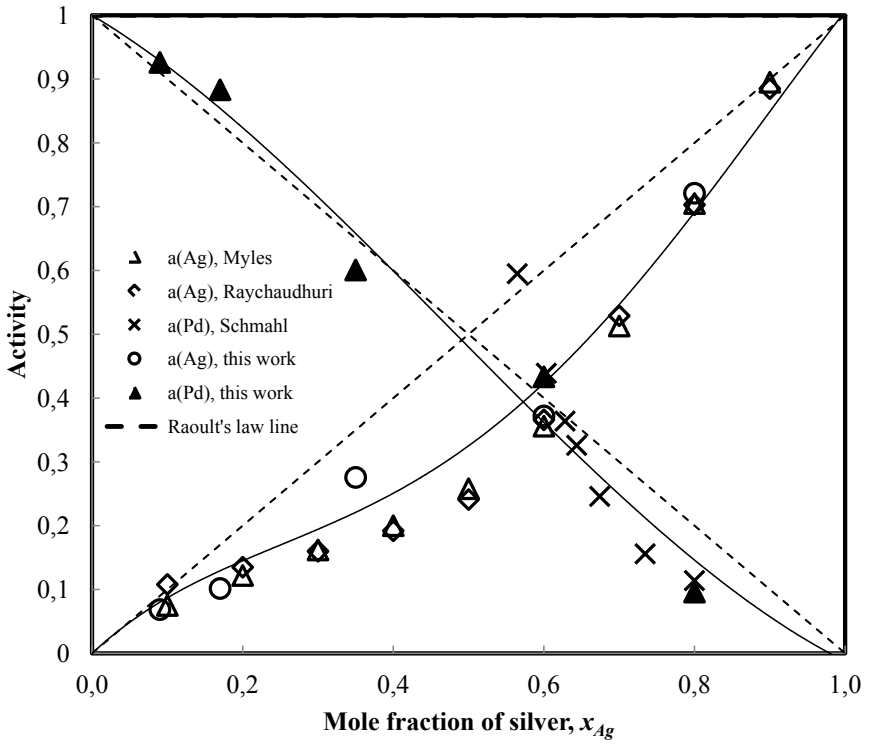

Fig. 5-1. Activities of silver and palladium in solid Ag-Pd alloys from various authors; the standard states are pure solid fcc Ag and Pd, where○ represents activity of silver at 600 K, ▲ represents activity of palladium at 600 K, × Schmahl [55] at 956 K,△ Myles et al. [53] at 1200 K and◇ Raychaudhuri [9], respectively.

The activities of palladium in the silver-rich alloys are found to have a negative deviation from Raoultian behavior, while in the palladium-rich alloys they show positive deviations from the ideal Raoultian behavior. The activity data of palladium obtained by the Gibbs-Duhem equation in the present study shows good agreement with the measured activity

of palladium by Schmahl [55] by the chemical equilibria method. The results also essentially confirm the data of Myles [53].

5.3 Thermodynamic properties

Fig. 5-2 shows the integral enthalpies of solution obtained in this study. The results show that the minimum integral enthalpies of mixing of Ag-Pd alloy is located at 60 at.% Ag, which essentially confirms the previous study by Chan and Hultgren [51], Luef et al. [52] and Myles [53].

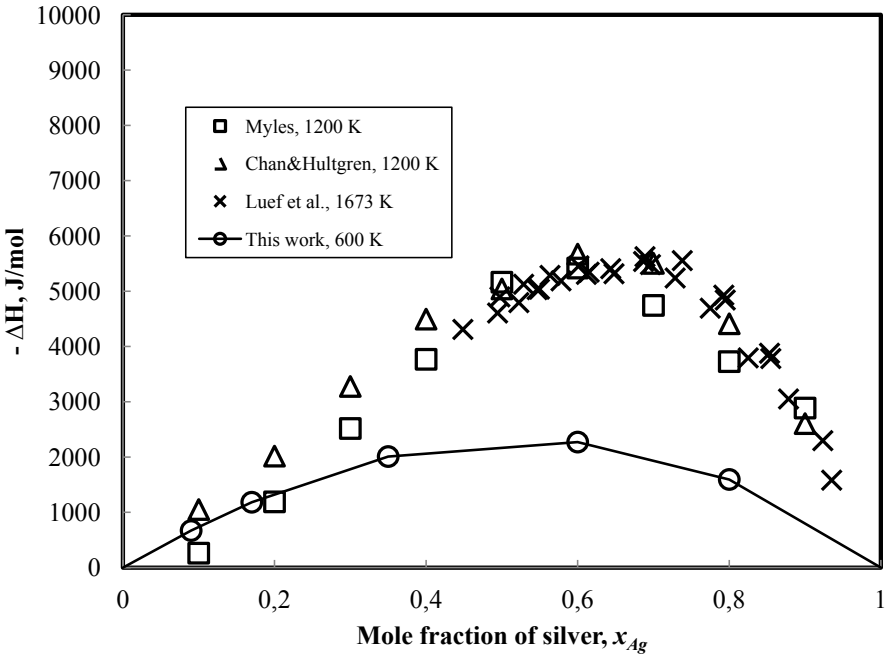

Fig. 5-2. Integral enthalpies of mixing of solid Ag-Pd alloys according to various authors, with pure silver and pure palladium as the standard states

It can be also seen that the enthalpies of mixing are less negative than those reported by Chan and Hultgren [51], Luef et al. [52] and Myles [53]. It can be attributed to the low temperature range of the present investigation in the solid state at 600 K, while other experiments were done in liquid alloys at 1200 K [51] and 1673 K [52].

6. Discussion

The thermodynamic properties of Ag-Au-Se ternary and Ag-Pd binary systems have been successfully measured by the advanced EMF method in this study.

6.1 Evaluation of the thermodynamic data

Table 6-1 shows the standard Gibbs energy and enthalpy of formation and entropy of Ag_2Se, AuSe and Ag_3AuSe_2, from both the data obtained in this study and the literature. The thermodynamic data obtained from this study show good agreement with the data from the literature with sound accuracy. The evaluation of the thermodynamic data from Ag-Pd system has been discussed in chapter 5.

Table 6-1. Standard thermodynamic properties of phases in Ag-Au-Se system

Compound	$-\Delta_f G^\circ / \mathrm{kJ \cdot mol^{-1}}$	$S^\circ / \mathrm{J \cdot K^{-1} mol^{-1}}$	$-\Delta_f H^\circ / \mathrm{kJ \cdot mol^{-1}}$	Reference
α- Ag_2Se	49.47±0.13	144.99±0.56	42.73±0.29	Osadchii [39]
α- Ag_2Se	48.90±1.0	148.20	42.70	Nasar [17]
α- Ag_2Se	49.59	149.20	43.09	Osadchii [20]
α- Ag_2Se	49.24±0.46	154.60±0.22	40.87±0.58	[Publication I]
β - Ag_2Se	47.43±0.29	169.01±0.78	35.02±0.48	Osadchii [39]
β - Ag_2Se	47.58	169.44	35.04	Osadchii [20]
β - Ag_2Se	47.64	169.57	35.06	[Publication I]
Ag_3AuSe_2	86.451±0.32	290.80±1.26	77.172±0.611	[39]
Ag_3AuSe_2	86.344±1.268	302.946±1.019	72.941±1.336	[Publication II]
β-AuSe	-	80.75	7.95	[22]
β-AuSe	4.11±1.30	75.49±3.55	8.36±1.83	[39, 67]
α-AuSe	-	86.61	3.77	[22]
α-AuSe	6.32	80.75	9.01	[68]
α-AuSe	9.626	75.730	13.807	[69]
α-AuSe	3.99	-	-	[67]
α-AuSe	5.43±0.56	78.15±2.14	8.77±1.31	[Publication III]

6.2 EMF method as an experimental tool

The advantages of EMF method result from its high accuracy and direct acquisition of Gibbs energy. Owing to the rapid development of the electronics, the accuracy of EMF method has been improved significantly in this study, which can reach 0.01 mV for each temperature. This means that the accuracy of Gibbs energy can reach the magnitude of Joules. The equilibria are ensured through the stable EMF reading obtained at the final stage of each run. The least squares analysis can give the temperature dependence of the cell reaction, which also provides an estimation of the uncertainties.

6.3 Impact of this work

The thermodynamic properties of the Ag-Au-Se system are crucial for copper anode slimes smelting. In the raw anode slimes, gold occurs mainly as tiny particles of metallic gold, which are commonly attached to selenide particles. Some gold is also present in the selenide form. Decopperizing the anode slimes retains much of the metallic gold, but also promotes the incorporation of gold in the structure of silver rich selenide species. A greater fraction of the gold is converted to $(Ag,Au)_2Se$ or Ag_3AuSe_2 when high-Se and high-Ag anode slimes are decopperized at elevated temperatures and pressures. After pelletization and roasting of the slimes, the gold is converted to a (Ag,Au)-alloy and Ag_3AuSe_2. Smelting of the roaster products eliminates the selenium and converts the gold to a silver-rich (Ag,Au,Pd)-alloy of doré Metals. Paper I to III show the thermodynamic stability of the Ag_2Se, AuSe and Ag_3AuSe_2 compounds, which are significant for the design of the copper anode slime refining process. The thermodynamic properties in the Ag-Pd system can help us understand the behavior of Ag-Pd alloy, which has various industrial applications, such as hydrogen permeation [41], hydrogen storage [42] and lead-free soldering [43].

Moreover, this study has provided an advanced experimental tool for thermodynamic measurement. The accuracy of the EMF method has been significantly improved by a gas purification system and temperature measurement. The state-of-the-art EMF method can be applied for thermodynamic investigation of other alloys and compounds.

6.4 Future work

The EMF method has shown its capacity as a powerful experimental tool for thermodynamic measurement for stoichiometric alloy and compounds. However, for non-stoichiometric materials, it would be time consuming for the EMF method to be used. Therefore, the further development of EMF method for non-stoichiometric compounds would be a research topic for future work.

In addition, computational thermodynamic method, such as CALPHAD (CALculation of PHAse Diagrams) and the first principle calculation, could be combined and would provide a high throughput thermodynamic investigation method. This can be another research topic for future work.

7. Conclusions

In this study, the thermodynamic properties of Ag_2Se, Ag_3AuSe_2 (fischesserite) and AuSe have been determined by the EMF method with AgI and $RbAg_4I_5$ as solid electrolytes. The equilibrium temperature of polymorphic phase transformation from α- Ag_2Se to β - Ag_2Se is determined in this work experimentally to be 407.7 K, by interpolation of the EMF vs. Temperature data. The enthalpy of phase transformation is 6.06 $kJ \cdot mol^{-1}$. The current experimental data suggest that a phase transformation of Ag_3AuSe_2 has been observed at 349.3 K. The temperature was obtained by solving the experimental EMF functions and taking into account the α-β solid state phase transformation of Ag_2Se at 407.7 K. The enthalpy of the phase transformation based on the EMF vs. temperature plot is 5.358±0.764 $kJ \cdot mol^{-1}$. At high temperatures, the polymorphic transformation from α'-Ag_3AuSe_2 to β-Ag_3AuSe_2, was observed in the EMF vs. T behavior of the experimental cell. It was determined to occur at 543 K.

Thermodynamic properties of Ag-Pd alloys, were obtained over a temperature range of 400-700 K. The activities of silver exhibit fairly large negative deviations from the ideal Raoultian behavior over most of the composition range. A small positive deviation from Raoultian behavior is found for low-silver alloys, which confirm the results from Raychaudhuri [49]. The activities of palladium in the silver rich alloys are characterized by negative deviations from the Raoult's law, while in the palladium rich alloys they show positive deviations. The activity data of palladium obtained in this study by the Gibbs-Duhem equation show a good agreement with the measured activity of palladium reported by Schmahl [55]. The integral enthalpies of mixing obtained in this study at 600 K show the minimum integral enthalpy of mixing of Ag-Pd alloys is located at 60 at.% Ag.

The EMF method has been improved by advanced cell design, a gas purification system, as well as temperature measurement, which can be used as an experimental tool for thermodynamic measurement for other alloys and compounds. The further development of the EMF method for non-stoichiometric compounds would be a research topic for future work.

8. References

[1] The White House (2011) Materials Genome Initiative.

[2] Moser Z, Fitzner K (1999) Thermochim Acta 332:1

[3] Ipser H, Mikula A, Katayama I (2010) Calphad 34:271

[4] Xu R, Husmann A, Rosenbaum T et al (1997) Nature 390:57

[5] Husmann A, Betts J, Boebinger G et al (2002) Nature 417:421

[6] Wiggett S, Swinbourne D, Eric R et al (1999) Metallurgical and Materials Transactions B-Process Metallurgy and Materials Processing Science 30:589

[7] Bellati M, Lussana S (1890) Att. Inst. Veneto 5:282

[8] Rahlfs P (1936) Z. Phys. Chem B31:157

[9] Earley J (1950) Am Mineral 35:337

[10] Wiegers G (1971) Am Mineral 56:1882

[11] Banus MD (1965) Science 147:732

[12] Shukla AK, Sen P, Sharma DD (1982) 86:198

[13] Grønvold F, Stølen S, Semenov Y (2003) Thermochimica Acta 399:213

[14] Scardala P, Piacente V, Ferro D (1990) Journal of the Less-Common Metals 162:11

[15] Kiukkola K, Wagner C (1957) J Electrochem Soc 104:379

[16] Takahashi T, Yamamoto O (1970) J Electrochem Soc 117:1

[17] Nasar A, Shamsuddin M (1997) Metallurgical and Materials Transactions B 28:519

[18] Oehsen V, Schmalzried H (1981) Berichte Der Bunsen-Gesellschaft-Physical Chemistry Chemical Physics 85:7

[19] Beck G, Janek J (2004) Solid State Ionics 170:129

[20] Voronin M, Osadchii E (2011) Russian J Electrochem 47:420

[21] Cranton G, Heyding R (1968) Canadian Journal of Chemistry 46:2637

[22] Rabenau A, Rau H, Rosenste G (1971) Journal of the Less-Common Metals 24:291

[23] Olin A, Nolang B, Ohman L et al (2005) Chemical thermodynamics of selenium, Elsevier

[24] Rabenau A, Schulz H (1976) Journal of the Less Common Metals 48:89

[25] Cretier JE, Wiegers GA (1973) Mater Res Bull 8:1427

[26] Wagner FE, Palade P, Friedl J et al (2010) International Conference on the Applications of the Mossbauer Effect (Icame 2009) 217

[27] Lee W, Jung D (1999) Bull Korean Chem Soc 20:147

[28] Ettema ARHF, Stegink TA, Haas C (1994) Solid State Commun 90:211

[29] Massalski TB, Okamoto H, Subramanian PR, L. Kacprzak (ed) (1990) Binary Alloy Phase Diagrams, 2nd Edition edn. ASM International

[30] Johan Z, Kvacek M, Picot P et al (1971) Bulletin De La Societe Francaise Mineralogie Et De Cristallographie 94:381

[31] Bindi L, Cipriani C (2004) Canadian Mineralogist 42:1733

[32] Wiegers G (1976) Journal of the Less-Common Metals 48:269

[33] Sakai H, Ando M, Ichiba S et al (1991) Chem Lett:223

[34] Wagner F, Sawicki J, Friedl J et al (1992) Can Mineral 30:327

[35] Fang CM, de Groot RA, Wiegers GA (2002) Journal of Physics and Chemistry of Solids 63:457

[36] Tavernier BH, Vervecken J, Messien P et al (1967) Zeitschrift für anorganische und allgemeine Chemie 356:77

[37] Smit TJM, Venema E, Wiersma J et al (1970) Journal of Solid State Chemistry 2:309

[38] Petzow G (1988) Ternary alloys: a comprehensive compendium of evaluated constitutional data and phase diagrams. 1, Ag-Al-Au to Ag-Cu-P. VCH, Weinheim

[39] Osadchii EG, Echmaeva EA (2007) Am Mineral 92:640

[40] Owens BB, Argue GR (1967) Science 157:308

[41] Lewis F, Magennis J, Mckee S et al (1983) Nature 306:673

[42] Picard C, Kleppa O, Boureau G (1979) J Chem Phys 70:2710

[43] Ghosh G, Kantner C, Olson GB (1999) Journal of Phase Equilibria 20:295

[44] Ruer R (1906) Zeitschrift für anorganische Chemie 51:315

[45] McKeehan LW (1922) Phys Rev 20:424

[46] Coles B (1956) Journal of the Institute of Metals 84:346

[47] Hoare FE, Yates B (1957) Proceedings of the Royal Society of London Series A Mathematical and Physical Sciences 240:42

[48] Pratt JN (1960) Trans Faraday Soc 56:975

[49] Raychaudhuri PK (1971) PhD Dissertation, Northwestern University

[50] Oriani R, Murphy WK (1962) Acta Metallurgica 10:879

[51] Chan JP, Hultgren R (1969) The Journal of Chemical Thermodynamics 1:45

[52] Luef C, Paul A, Flandorfer H et al (2005) J Alloys Compounds 391:67

[53] Myles KM (1965) Acta Metallurgica 13:109

[54] Eremenko VN, Lukashenko GM, Pritula VL (1968) Russ J Phys Chem 42:346

[55] Schmahl NG (1951) Zeitschrift für anorganische und allgemeine Chemie 266:1

[56] Savitskii EM, Pravoverov NL (1961) Russ J Inorg Chem 6:253

[57] Karakaya I, Thompson WT (1988) Bulletin of Alloy Phase Diagrams 9:237

[58] Sopoušek J, Zemanová A, Vřešťál J et al (2010) J Alloys Compounds 504:431

[59] Burley G (1963) Am Mineral 48:1266

[60] Turbant C, Lorenz E (1914) Zeitschrift für Physikalische Chemie 87:513

[61] Patterso JW (1971) J Electrochem Soc 118:1033

[62] Tesfaye F, Taskinen P (2014) Journal of Solid State Electrochemistry 18:1683

[63] Hull S, Keen DA, Sivia DS et al (2002) Journal of Solid State Chemistry 165:363

[64] Geller S (1967) Science 157:310

[65] Bradley J, Greene P (1967) Transactions of the Faraday Society 63:424

[66] Rom I, Sitte W (1997) Solid State Ionics 101:381

[67] Echmaeva EA, Osadchii EG (2005) Geochemistry, Mineralogy and petrology 43:75

[68] Knacke O, Kubaschewski O, Hesselmann K (1991) Thermochemical properties of inorganic substances, Second edition. Springer-Verlag

[69] Ihsan Barin (1989) Thermochemical data of pure substances, Wiley, Weinheim

Appendices

Table A-1. Experimental EMF values in Ag-Se system

T, K	E, mV
465.3	283.61
455.5	281.41
445.8	279.22
426.2	274.93
406.9	270.70
404.0	270.06
402.0	269.63
392.5	268.08
368.5	264.85
359.1	263.74
349.7	262.41
350.4	262.05
360.0	264.03
369.6	265.85
379.3	267.06
389.0	267.98
398.7	269.13
408.4	271.02
418.2	273.12
427.9	275.22
437.7	277.32
447.5	279.43
457.3	281.59
467.2	283.80
477.0	286.12
486.9	288.24
496.8	290.13

Table A-2: Experimental EMF values for Ag-Au-Se system

T, K	E, mV
298.0	125.96
302.8	126.42
307.6	127.02
312.3	127.27
317.1	127.94
321.8	128.10
326.6	128.79
331.4	129.18
336.2	130.26
340.9	131.05
345.9	131.55
350.5	133.29
355.6	133.41
360.2	135.56
365.2	133.67
369.8	137.97
375.0	136.51
379.5	140.42
384.6	139.45
389.2	142.82
394.2	142.61
394.3	143.50
396.7	144.29
399.0	145.71
403.9	146.95
404.1	147.81
406.7	149.11
408.7	149.44
413.8	152.38
418.4	153.90
418.4	153.70
421.4	155.93
423.6	156.94
428.2	158.82
433.4	161.77
438.0	163.68
438.0	163.68
441.2	164.03
443.2	166.91
447.9	169.53

451.1	169.29
451.7	171.48
457.7	175.03
460.8	175.02
465.9	178.57
467.5	181.49
470.8	181.23
475.8	184.85
477.4	188.04
480.7	188.08
485.7	191.63

Table A-3. Experimental EMF values in Au-Se system

T, K	E, mV
434.1	288.18
441.9	289.12
451.7	291.16
462.5	292.82
473.1	293.98
483.7	296.16
492.6	297.74
502.8	298.96
514.0	301.38
524.7	304.78
535.3	305.00
545.6	307.91
556.6	311.38
567.7	315.37
578.3	319.20
588.9	323.00
600.1	327.04
607.9	329.84
617.7	333.37
628.5	337.26
639.1	340.96
649.7	342.02
658.6	346.25
668.8	353.18
456.4	291.64

478.6	295.54
497.8	298.91
519.2	302.67
540.8	306.46
571.9	316.96
593.5	324.56
621.7	334.47
641.4	341.39

Table B-1. Experimental EMF values in $Ag_xPd_{(1-x)}$, when x=0.8

T, K	E, mV
696.8	18.95
746.3	20.01
647.0	17.62
547.8	16.24
597.3	16.52
696.7	18.68

Table B-2. Experimental EMF values in $Ag_xPd_{(1-x)}$, when x=0.6

T, K	E, mV
476.8	45.81
755.6	59.49
654.7	52.60
654.7	53.20
755.3	58.87

Table B-3. Experimental EMF values in $Ag_xPd_{(1-x)}$, when x=0.35

T,K	E,mV
654.8	70.73
554.0	62.33
503.7	60.46
553.9	61.55
604.2	66.72
654.6	71.96

Table B-4. Experimental EMF values in $Ag_xPd_{(1-x)}$, when x=0.17

T,K	E,mV
654.7	123.36
604.5	116.99
554.0	115.04
503.8	111.32
453.6	104.74

Table B-5. Experimental EMF values in $Ag_xPd_{(1-x)}$, when x=0.09

T/K	E/mV
644.6	143.16
545.3	134.10
446.4	127.87
495.6	128.76
545.2	133.62
594.9	137.61

Errata

Publication I

- $\Delta\bar{G}_{Ag_2Se}$, $\Delta\bar{H}_{Ag_2Se}$ and $\Delta\bar{S}_{Ag_2Se}$ should be $\Delta_f G_{Ag_2Se}$, $\Delta_f H_{Ag_2Se}$ and $\Delta_f S_{Ag_2Se}$ for equation (1) to equation (11) .
- In Table 2, $\Delta\bar{G}$, $\Delta\bar{H}$ and $\Delta\bar{S}$ should be $\Delta_f G^0_{298}$, $\Delta_f H^0_{298}$ and S^0_{298}.
- In addition, $\Delta_f H^0_{298}$ for α- Ag_2Se has been modified, as well as the data for β - Ag_2Se by Nasar and Shmsuddin [14].

Table 2. A comparison of values of the standard thermodynamic properties of Ag_2Se

Compounds	$-\Delta_f G^0_{298}$, kJ/mol	S^0_{298} J · K^{-1}mol^{-1}	$-\Delta_f H^0_{298}$, kJ/mol	References
α- Ag_2Se	49.47±0.13	144.99±0.56	42.73±0.29	Osadchii and Echmaeva [21]
α- Ag_2Se	48.90±1.0	148.20	42.70	Nasar & Shamsuddin [14]
α- Ag_2Se	49.59	149.20	43.09	Voronin and Osadchii [17]
α- Ag_2Se	49.24±0.46	154.60±0.22	40.87±0.58	This work
β - Ag_2Se	47.43±0.29	169.01±0.78	35.02±0.48	Osadchii and Echmaeva [21]
β - Ag_2Se	47.58	169.44	35.04	Voronin and Osadchii [17]
β - Ag_2Se	47.64±0.07	169.57±1.53	35.06±0.099	This work

Publication II

- Equations (17) and (19) have been modified as

$$\Delta_f G^{\circ}(\alpha - Ag_3AuSe_2) = 2\Delta_f G^{\circ}(\alpha - Ag_2Se) - \Delta_r G^{\circ}(Ag_3AuSe_2) \quad (17)$$

$$\Delta_f H^{\circ}(\alpha - Ag_3AuSe_2) = 2\Delta_f H^{\circ}(Ag_2Se) - \Delta_r H^{\circ}(Ag_3AuSe_2) \quad (19)$$

- The enthalpy of the phase transformation of Ag_3AuSe_2 should be 5.358 kJ/mol in the conclusion.

Publication V

- $a_{Ag[Pd]}$ is the activity of silver in silver palladium alloy in equation (6).
- ΔG_{Ag}, ΔS_{Ag} and ΔH_{Ag} shall be $\Delta\bar{G}_{Ag}$, $\Delta\bar{S}_{Ag}$ and $\Delta\bar{H}_{Ag}$ in equations (8-12) and Table 4, and ΔH^M_{Ag}, ΔH^M_{Pd}, ΔG^M_{Ag}, ΔG^M_{Pd}, ΔS^M_{Ag} and ΔS^M_{Pd} shall be $\Delta\bar{H}^M_{Ag}$, $\Delta\bar{H}^M_{Pd}$, $\Delta\bar{G}^M_{Ag}$, $\Delta\bar{G}^M_{Pd}$, $\Delta\bar{S}^M_{Ag}$ and $\Delta\bar{S}^M_{Pd}$ in equations (18-22).
- Table 4 has been modified as following,

Aalto-DD 172/2014

ISBN 978-952-60-5934-1 (printed)
ISBN 978-952-60-5935-8 (pdf)
ISSN-L 1799-4934
ISSN 1799-4934 (printed)
ISSN 1799-4942 (pdf)

Aalto University

Department of Materials Science and Engineering
www.aalto.fi

BUSINESS +
ECONOMY

ART +
DESIGN +
ARCHITECTURE

SCIENCE +
TECHNOLOGY

CROSSOVER

**DOCTORAL
DISSERTATIONS**